

## Sulfide-passivated GaAs (001). II. Electronic properties

D. Paget and A. O. Gusev\*

*Laboratoire de Physique de la Matière Condensée, Ecole Polytechnique, 91128 Palaiseau, France*

V. L. Berkovits

*A. F. Ioffe Physico-Technical Institute, 194021 Saint Petersburg, Russia*

(Received 30 May 1995)

We have investigated the correlation between the change of the surface electronic properties (surface recombination velocity, surface barrier) and the change of the surface chemical bonds under annealing in ultrahigh vacuum of sulfide-passivated (001)GaAs. The electronic properties of a  $(\text{NH}_4)_2\text{S}$ -passivated surface were monitored using room-temperature photoreflectance, which gave the value of the surface barrier, and photoluminescence. The surface chemical bonds were probed by (i) reflectance anisotropy spectroscopy, which essentially monitors the optical transitions due to surface dimers, and (ii) core-level spectroscopy results on the same sample (companion paper in the same issue). We find that breaking of arsenic-related chemical bonds, which induces arsenic dimers on the surface, produces an increase of photoluminescence intensity (PLI). Conversely, a clear correlation is found between the desorption of sulfur due to breaking of Ga-S chemical bonds, the appearance of the gallium dimer line, and the decrease of PLI. Based on these results, we outline the dominant features of sulfide passivations: (i) The improvement of electronic properties of (001) GaAs arises due to formation of S-Ga bonds on the gallium-terminated part of the surface, (ii) electronic properties of the as-treated surface are deteriorated by excess arsenic, which produces midgap levels, and (iii) the passivation efficiency can also be reduced by formation of additional surface defects due to etching of the surface in sulfide solutions.

### I. INTRODUCTION

Several years ago, treatment of GaAs surfaces by sulfide solutions had been shown to produce a strong increase of the photoluminescence intensity (PLI), which triggered a wealth of studies.<sup>1-7</sup> Some of them investigated the electronic properties of the passivated surface. It was found that, although the photoluminescence intensity increases, the surface Fermi level is still pinned, as a significant surface barrier exists.<sup>3,4</sup> Other studies were devoted to the chemical aspects of this passivation, mainly the chemical bonds between sulfur and the substrate atoms, using x-ray photoemission spectroscopy (XPS),<sup>3,5-7</sup> and the modifications of these properties under exposure to ambient air.

Up to now, there has been no experimental correlation between the chemical and electronic surface properties of sulfide-passivated GaAs. As a result, the fundamental microscopic mechanism for the improvement of the surface electronic properties is still unknown. One of the reasons is that the nature of the surface states in the forbidden gap of (001)GaAs which determine the surface electronic properties is not known precisely. Quite generally these states can be (i) extrinsic or intrinsic surface defects, (ii) related to the presence of the foreign atoms (for example, oxygen), or (iii) due to some overlayer covering the semiconductor (for example, containing excess or elemental arsenic).

There exist several theoretical models which explain the electronic properties of sulfide-passivated surfaces. First, tight-binding calculations for the system S-GaAs have shown that the electronic passivation could be due to the establishment of S-Ga chemical bonds, for which the bonding and antibonding levels are found to be out of the forbidden gap.<sup>8</sup>

This is in contrast to S-As chemical bonds, which do not reduce the density of surface states in the gap. Another explanation relates the modification of the surface electronic properties to an indirect change of surface chemistry during passivation. Spindt and co-workers<sup>3,9</sup> have proposed that the change of surface recombination velocity (SRV) and surface barrier is due to the modification of surface arsenic antisite concentration during passivation. The increase of the PLI after sulfide passivation can also depend on other less fundamental phenomena, such as the removal of surface oxides. Moreover, the morphology of the surface is probably modified, as passivating solutions have been found to produce etching of the surface.<sup>10</sup> This could also change the surface recombination velocity through the modification of roughness or surface defect concentration.

The present work is, to our knowledge, the first analysis of the experimental correlation between the electronic properties of the surface and the chemical bonds on this surface. We selectively break surface chemical bonds by annealing in ultrahigh vacuum (UHV) at increasingly high temperatures. We have shown in a previous work that the correlated investigation of reflectance-anisotropy spectroscopy (RAS) and core-level spectra allows us to understand the nature of chemical bonds which are broken by these annealings.<sup>11</sup> In the present work, we monitor the effect of the same annealings on the surface barrier and surface recombination velocity.

### II. PRINCIPLES AND EXPERIMENT

The electronic properties are analyzed using band-to-band photoluminescence, and using photoreflectance (PR). This

last technique allows us to control the surface barrier.<sup>12</sup> The surface chemical properties are analyzed using Auger electron spectroscopy (AES) and RAS. For the (001) surface, this technique measures the quantity

$$\frac{\Delta R}{R} = \frac{R_{[\bar{1}\bar{1}0]} - R_{[110]}}{R}, \quad (1)$$

which is the relative difference between the near-normal reflectivities for light polarized along the  $[\bar{1}\bar{1}0]$  and  $[110]$  directions of the semiconductor surface and  $R$  is their mean value. Due to the fact that the bulk contribution is the same for these polarizations, this contribution is cancelled out in the RAS signal. Thus, RAS is a probe of the optical transitions on the clean GaAs(001) surface, which originate essentially from gallium dimers or arsenic dimers, depending on the surface reconstruction.<sup>13</sup> As demonstrated in our UPS/RAS study,<sup>11</sup> this allows us to investigate surface chemistry, simply because the breaking of chemical bonds upon annealing induces the formation of additional dimers, which are then revealed from a change in the RA spectrum.

All measurements were carried out at room temperature in an UHV chamber, with a base pressure in the low  $10^{-11}$  mbar range. Our experiment is equipped (i) with a RAS system, described elsewhere;<sup>14</sup> (ii) with a standard PR setup. We recall that this technique consists of measuring the reflectance variation of a probe beam caused by the additional excitation of the sample by a pump beam, which induces photovoltage effects and modifies the surface barrier. Here the pump source was a krypton laser (2.2 eV) with a power density of approximately 20 mW/cm<sup>2</sup>; PR analysis was performed with the same probe source as RAS, and with a silicon photodiode as the light detector. To avoid the photovoltaic effect, we used a very small probe power density of about 2  $\mu$ W/cm<sup>2</sup>, and we verified that the pump power density, of a fraction of a mW/cm<sup>2</sup>, was sufficiently small. For both experiments, synchronous detection techniques were used, with for PR a very small light modulation frequency (11 Hz) in order to allow recharging of surface recombination centers; (iii) with a PL setup, using the same excitation laser with an excitation power density of 200 mW/cm<sup>2</sup>. The PL signal is detected by a cooled GaAs photomultiplier through a Jobin-Yvon H20 spectrometer. Careful control of the experimental conditions, and in particular of the sample temperature after cooling, allowed us to monitor the PL intensity with a precision better than 5%.

These measurements were all performed through the same viewpoint, without changing the sample position, by using movable mirrors to select the appropriate light detector. Our experiment is also equipped with an Auger spectrometer. The incident electron energy is 3 keV. We used AES to monitor after each annealing stage the residual impurity concentration as well as the sulfur concentration on the surface. We used the tabulated sensitivities to derive the ratio of these concentrations to the gallium one.

For this study, we used the same sample and preparation procedure as for our UPS/RAS investigation.<sup>11</sup> The annealing stages, described in Table I, are also similar. We recall that our sample is a *p*-type GaAs epitaxial layer of acceptor concentration in the  $10^{16}$  cm<sup>-3</sup> range, grown at Laboratoire Central de Recherches, Thomson CSF, on a (001) substrate

TABLE I. Runs corresponding to the various annealing temperatures for the (NH<sub>4</sub>)<sub>2</sub>S-passivated sample. Run 1 corresponds to the as-treated surface, before any annealing.

Temperature of annealing	Run number
as-treated (30 °C)	1
150 °C	2
250 °C	3
270 °C	4
360 °C	5
520 °C	6
520 °C second	7
520 °C third	8
550 °C	9

disoriented by approximately 2° towards the (110) orientation. The passivation procedure consisted in a 5-min treatment by a fresh 0.75M solution of (NH<sub>4</sub>)<sub>2</sub>S at 60 °C, followed by a rapid deionized-water rinsing and an isopropanol rinsing, after which the sample was immediately introduced into the experiment through an introduction lock via an oxygen-free glove box.

The RA spectra are shown in Fig. 1: (i) the spectrum of the as-treated surface is a broad spectrum where, if present, dimer signals cannot simply be isolated. This reveals the fact that our sample is covered by a relatively thick passivating overlayer, which saturates any dangling bond on the semiconductor surface. Subsequent annealing stages, up to 270 °C, have been shown to give rise<sup>11,15</sup> to the gradual desorption of this passivating overlayer, after which the sample is covered by essentially a monolayer of atoms. (ii) Annealing at 360 °C produces the appearance of the characteristic arsenic dimer signal, as revealed by the rise of the RA signal near 3 eV. It means that, after this annealing, bonds involving surface arsenic begin to break. Our previous study<sup>11</sup> shows that this is due essentially to the desorption of excess arsenic from this surface. (iii) Annealing at 520 °C has been shown to produce sulfur desorption from the surface.<sup>11</sup> Here, we performed three distinct annealings at this temperature in order to progressively desorb the sulfur atoms from the surface. Shown in Fig. 1 are the RA spectra after the first two annealings at 520 °C. One observes the appearance and the rise of the negative gallium line at 2.2 eV. As shown from our UPS measurements and verified here using AES, the gallium dimers appear due to the breaking of chemical bonds between surface gallium and sulfur.

The above RA spectra are identical to those of our preceding investigation,<sup>11</sup> which shows that the chemistries of the two surfaces are, as expected, identical. More precisely, we find that the annealing stage at 520 °C of the preceding investigation rather corresponds with the annealing stage at 550 °C of the present work, which we attribute to slight differences in the temperature measurements. Also, there are small differences in the corresponding RA spectra for the annealing stages up to 270 °C. These reflect possible differences in the passivating overlayer, due to slightly different environments during the sample introduction into the experi-

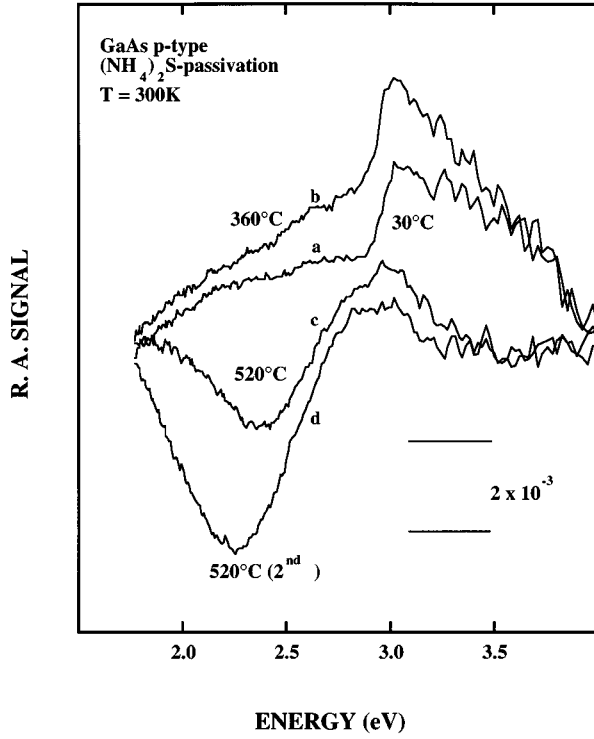


FIG. 1. Reflectance anisotropy spectra at room temperature of  $(\text{NH}_4)_2\text{S}$ -passivated GaAs. Curve (a) corresponds to the as-treated sample, curves (b)–(d) correspond to spectra taken after successive annealings at temperatures indicated between parentheses.

ment. Due to the small magnitude of these effects, it is perfectly justified to use the present technique as a bridge between the two works.

We now describe the measurement of the surface electronic properties. The PR spectra obtained after annealing at 270 and 520 °C are shown as an example in Fig. 2. Apart from the excitonic effect<sup>16</sup> near 1.42 eV these spectra exhibit Franz-Keldysh oscillations (FKO) above the band gap, the extrema of which can be used to determine the magnitude of the surface electric field by using the following expression:<sup>12</sup>

$$n\pi = \varphi + \frac{4}{3} \left( \frac{E_n - E_g}{\hbar\theta} \right)^{3/2}, \quad (2)$$

where  $n$  is the index of the  $n$ th extremum,  $\varphi$  is an arbitrary phase,  $E_n$  is the energy position of the  $n$ th extremum,  $E_g$  is the energy gap (1.42 eV), and  $\hbar\theta$  is the electro-optical energy:<sup>12</sup>

$$(\hbar\theta)^{3/2} = \left( \frac{q\hbar F_{dc}}{2\mu} \right)^{1/2}, \quad (3)$$

where  $\mu$  is the reduced interband effective mass for electron and heavy-hole pairs, and  $q$  is the electronic charge. Thus, this measurement gives us the surface electric field  $F_{dc}$  in the absence of pump excitation, provided the photovoltage is not too large. The change of this electric field between the two annealing stages is clearly seen from the distinct positions of these extrema for the two spectra. Plotted in the insert of Fig. 2 is the quantity  $(4/3\pi)(E_n - E_g)^{3/2}$  as a function of index  $n$ . The slope of the fitted lines gives directly the electric field

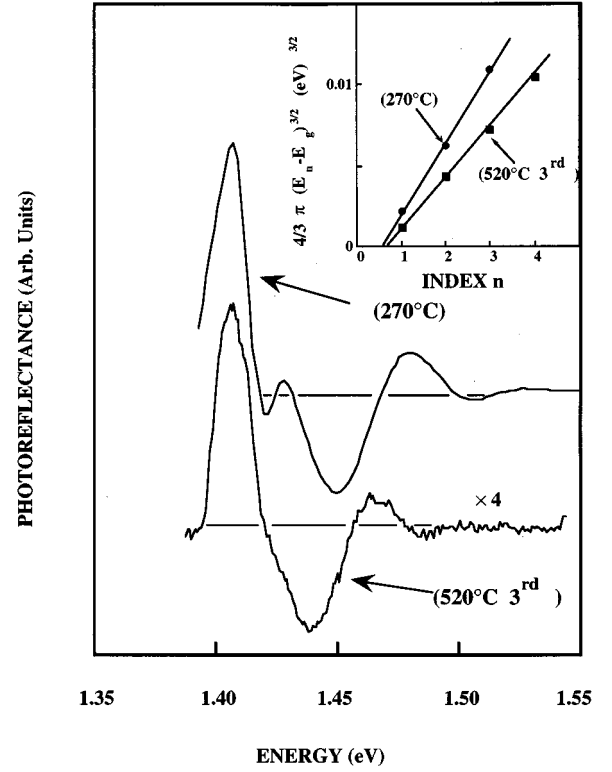


FIG. 2. Photoreflectance spectra at room temperature of  $(\text{NH}_4)_2\text{S}$ -passivated GaAs after annealing at 270 and 520 °C. The insert shows the treatment which allows us to obtain the surface electric field using the positions of the extrema of the spectrum (see text).

$F_{dc}$  [Eq. (3)]. Finally, we have obtained the Fermi-level position on the surface by using for calibration the same wafer with an oxidized surface, for which the pinning position is known.<sup>17</sup> This measurement also gives the acceptor concentration of our sample, which we find equal to  $8 \times 10^{15} \text{ cm}^{-3}$ .

Note that in Fig. 2 the photoreflectance amplitude (PRA), defined as the difference between the signal maximum and minimum over the spectrum, changes with annealing. It has been shown that the PRA is a function of  $F_{dc}$  as well as of the variation of the surface field  $F_{ac}$  produced by the modulated laser excitation:<sup>12</sup>

$$\text{PRA} \sim F_{dc}^{1/3} F_{ac}. \quad (4)$$

Using standard theory, we express the PRA as a function of the surface barrier  $V_b$  in the dark, and its variation  $V_p$  under light excitation:

$$\text{PRA} \sim V_b^{2/3} (1 - \sqrt{1 - V_p/V_b}). \quad (5)$$

The photovoltage  $V_p$  can be calculated very simply. We first write the zero current condition through the surface, which yields a relationship involving the photocurrent density  $J_p$ :<sup>18</sup>

$$V_p = \frac{kT}{q} \ln \left[ \frac{J_p}{J_{sat}} \exp \left( \frac{qV_b}{kT} \right) + 1 \right], \quad (6)$$

where  $J_{\text{sat}}$  is the saturation current density, determined by thermionic emission and diffusion. The photocurrent density can be expressed in terms of both drift and diffusion components in the usual form:<sup>19</sup>

$$J_p = \frac{qI_L(1-R)}{\hbar\omega} \left( 1 - \frac{\exp(-\alpha W)}{1 + \alpha L_d} \right), \quad (7)$$

where  $I_L$  is the laser power density,  $\hbar\omega$  is the photon energy,  $R$  is the surface reflectivity,  $\alpha$  is the adsorption coefficient,  $W$  is the width of the space-charge layer, and  $L_d$  is a diffusion length of minority carriers. We point out that this last equation neglects the recombination current, so that this picture neglects any changes of SRV.

We finally discuss the PL investigation. We found that the shape of the PL spectrum is not modified by the annealing. We shall therefore, in the following, only consider integrated PL intensities. The value of PLI obtained using a standard resolution of the diffusion equation in the bulk of the semiconductor<sup>20</sup> is found to depend both on the surface barrier and on the SRV:

$$\text{PLI} \sim \frac{\exp[-(\alpha + \alpha_{\text{PL}})W]}{(\alpha_{\text{PL}}L_d + 1)(Z + 1)} \left( 1 + \frac{Z + \alpha_{\text{PL}}L_d}{1 + \alpha L_d} \right), \quad (8)$$

where  $\alpha_{\text{PL}}$  is the absorption coefficient at the PL wavelength,  $Z$  is related to the surface recombination velocity, and  $S$  by  $Z = SL_d/D_n$ , where  $D_n$  is the diffusion coefficient of minority carriers (electrons). The exponential term in Eq. (8) reflects the “dead-layer” model, which states that the space-charge region does not contribute to the PLI.

The experimental results are summarized in Fig. 3, which shows for all annealing stages the variation after annealing of the surface Fermi level (SFL) position of the PRA and of the PLI. These results are shown by full circles, with solid lines given as a guide for eye.

### III. CORRELATION BETWEEN SURFACE CHEMICAL BONDS AND ELECTRONIC PROPERTIES

We first discuss the effect of breaking of Ga-S bonds on the surface chemical properties. This breaking occurs under annealing at 520 °C as revealed from our surface-sensitive techniques: this annealing produces (i) a reduction of sulfur Auger signal, (ii) a decrease of the line related to Ga-S bonds in the Ga 3*d* core-level spectrum,<sup>11</sup> and (iii) the formation of gallium dimers, revealed from their optical signature in the RA spectrum. As shown in Fig. 4, this increase of the gallium dimer signal is very well correlated with the decrease of the sulfur Auger signal.

The outstanding effect of these annealings on the surface electronic properties is the decrease of the PL intensity. Note that these annealings do not induce any modification of the surface electric field. Thus, from Eq. (8), the PL variation can only be due to a change of surface recombination velocity, due to a modification of the density of surface recombination centers. More detailed analysis of these results can be made by comparing the PLI with the one of an oxidized sample of the same wafer, for which we take a value of the SRV of 10<sup>6</sup> cm/s.<sup>21</sup> Using Eq. (8), we find that the SRV increases by approximately a factor of 5 upon sulfur desorption. The values of the SRV for the various annealing stages,

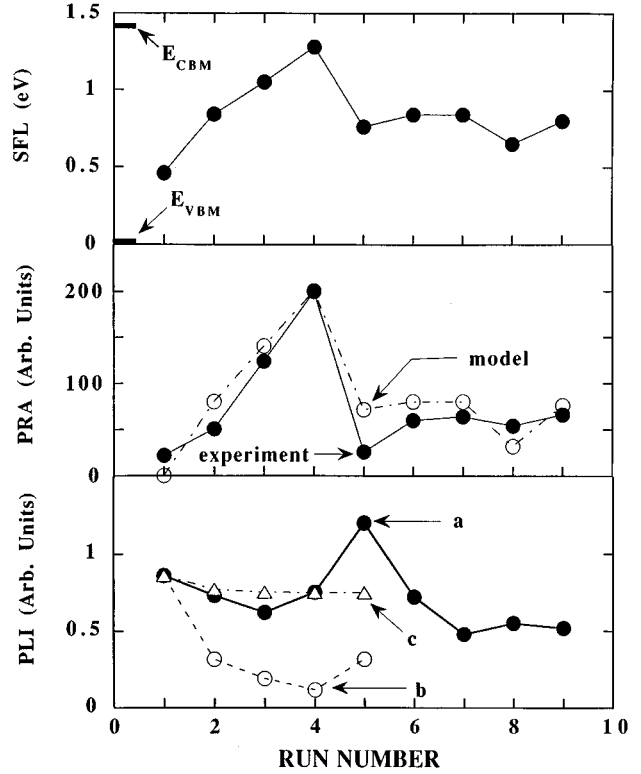


FIG. 3. Surface Fermi-level position relative to valence-band maximum (VBM) and conduction-band minimum (CBM), photoreflectance amplitude, and integrated photoluminescence intensity [curve (a)] as a function of run number for the (NH<sub>4</sub>)<sub>2</sub>S-passivated sample (all results are depicted by full circles, with solid lines given as a guide to the eye). The calculated PRA is depicted by open circles with dashed-dotted line. Also shown are two differently calculated values of PLI: by taking into account the photovoltaic effect, induced by laser irradiation [curve (c)], and by neglecting this one [curve (b)].

shown in Fig. 4, are found by estimating the minority carrier (electrons) diffusion length as 5 μm and lifetime as 1 ns.

The present results verify the theoretical prediction of Ohno and Shiraishi<sup>8</sup> that formation of the S-Ga surface bonds in bridge-site configuration does not induce a level in the band gap. The effect of the other possible modifications of the surface induced by this annealing cannot be correlated with the change of PLI: We find, as also shown elsewhere,<sup>11</sup> that a small amount of residual impurities is present on sulfide-passivated surfaces. However, the PLI change cannot be interpreted by the desorption of these residual impurities from the surface: Auger analysis shows that, after the first annealing stage at 520 °C, desorption of oxygen is complete and carbon concentration does not change, whereas PLI continues to decrease. Another annealing-induced surface modification is arsenic desorption, as shown from the decrease of the arsenic dimer signal. Again, this decrease essentially occurs at the first annealing stage at 520 °C, after which the modifications of the arsenic dimer line are much smaller.

For annealing stages to lower temperature, the results are very different, because the SFL position changes. Whereas the PLI allows us to capture the modification of the surface electronic properties due to annealing to 520 °C, the present

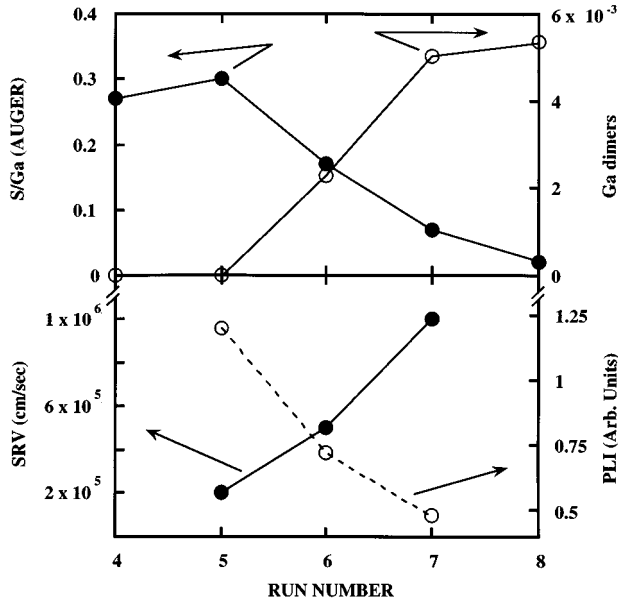


FIG. 4. Effect of sulfur desorption on the surface electronic properties upon successive annealings at 520 °C: This annealing induces the decrease of the S/Ga Auger signals and the increase of the intensity of gallium dimers, as found by RAS (upper part). The lower panel shows the variation of photoluminescence intensity, and of the calculated surface recombination velocity.

annealing stages only produce a limited PLI variation, the PRA variation being large.

In order to interpret these results, we have calculated using Eqs. (4)–(8) the modifications of both PRA and PLI induced by the *sole change of surface barrier*. In principle, the calculation of PRA requires the value of several parameters, which are not known precisely, such as the diffusion length  $L_d$  and to some extent the saturation current density  $J_{\text{sat}}$ . However, with the chosen value of the excitation energy, the absorption depth  $1/\alpha$  is much smaller than the width  $W$  of the depletion layer, so that the second term in Eq. (7) is small compared to 1, and  $J_p$  is independent of  $L_d$ , and is given by

$$J_p \approx \frac{qI_L(1-R)}{\hbar\omega}. \quad (9)$$

Furthermore, we have chosen the excitation power density so that the photovoltage is much larger than  $kT/q$ . Thus, using Eq. (6), this quantity can be approximated by the simple form

$$V_p \approx V_b + \frac{kT}{q} \ln\left(\frac{J_p}{J_{\text{sat}}}\right). \quad (10)$$

As a consequence, the value of the photovoltage does not depend on the values of saturation current  $J_{\text{sat}}$  and photocurrent  $J_p$ , but only on the order of magnitude of their ratio. Apart from these very weak dependences, the calculated PRA value only involves a scaling factor, which is then practically our only adjustable parameter.

We first analyze the effect of annealing up to 270 °C (annealing runs 2–4), which induces desorption of the passivating overlayer.<sup>11</sup> During this desorption, the SFL position is

found to rise from 0.5 eV above the valence band maximum (VBM) to 1.3 eV above this maximum. In the same way, the PRA strongly increases. The values of the PRA, calculated using Eqs. (4)–(7), are shown in Fig. 3 (dashed line). One can see that, indeed, the PRA changes can be very well explained by the modifications of the surface barrier. This also means that the SRV does not change significantly upon desorption of the overlayer.

In the same conditions, the PL intensity does not change significantly. Shown in the bottom panel of Fig. 3, along with the experimental results (a) is the PLI value calculated from Eq. (8), without taking into account the photovoltage (b). This calculated PLI, normalized to the experimental value for the as-treated surface, does not reproduce the experimental results. However, if we now take into account the dependence of  $W$  on the photovoltage (c), we find that the PLI variation is very small, which explains the experimental results for the annealing stages that we consider here. This shows that, in the same way as for the PRA, the PLI variation after annealing can be explained by the barrier change, so that the SRV essentially does not change.

The small PLI variation is due to the fact that, although the depletion layer width *in the dark* changes significantly, after annealing, the variation of this quantity *under light excitation* is small because of the compensating effect of the photovoltage. Indeed, as seen from Eqs. (9) and (10), the barrier  $V_b - V_p$  under light excitation stays almost constant if the barrier in the dark  $V_b$  is modified by the desorption of the overlayer. This desorption does not induce a significant change of the SRV, and therefore produces a negligible modification of the PLI, given by Eq. (8). This situation clearly takes place for runs 1–4 [curve (c) in Fig. 3], which indeed explains that, up to annealing at 270 °C, the PLI changes are much smaller than the PRA ones.

The effect of annealing at 360 °C, which induces arsenic dimers (annealing run 5), is different: The PLI increases, whereas the SFL position and PRA decrease. Using the above model, we find that the PRA decrease can be explained almost completely by the variation of the SFL position. On the other hand, the PLI increase cannot be interpreted by the sole variation of surface barrier because, as discussed above and shown in curve (c), this variation would predict an almost constant PLI value. We conclude that appearance of arsenic dimers induces both a variation of surface barrier and of SRV.

Thus, in the present case, photoreflectance and photoluminescence are complementary for the investigation of surface electronic properties: the SFL motion is revealed by the PRA and the positions of the extrema in the PR spectrum, whereas the PLI is weakly sensitive to the position of SFL. Conversely, the PLI reveals the change of SRV produced by S desorption, which in turn causes a minor modification of the PR spectrum.

The present study allows us to distinguish three main annealing stages in the evolution of the surface electronic properties. The desorption of the passivating overlayer, which occurs under annealing up to approximately 250 °C, produces a change of the surface barrier without strongly affecting the value of the SRV. Conversely, the final annealing stage at 520 °C, which induces desorption of sulfur from the surface and Ga dimers, results in a decrease of SRV without

strongly altering the SFL. Intermediate annealing, which induces As dimers due to breaking of As-related chemical bonds, results in an increase of SRV and a lowering of the SFL position to a value near midgap.

#### IV. DISCUSSION

We first discuss the behavior of the SFL. The results on the as-treated surface confirm previous findings according to which, for *p*-type GaAs, sulfide-passivation reduces the surface barrier.<sup>4</sup> To explain the downshift of SFL, in the framework of this model, Spindt and co-workers have proposed that the as-treated surface is depleted with arsenic.<sup>3,9</sup>

Although we cannot completely exclude this picture, it does not explain our results satisfactorily. In the framework of this model, it would be natural to interpret the Fermi-level motion during desorption of the passivating overlayer as due to an increase of excess arsenic concentration. This should manifest itself as an increase in the surface component due to excess arsenic in the As 3*d* core-level spectrum. However, we find that the desorption of the overlayer only increases the concentration of excess arsenic after the first annealing stage at 150 °C.<sup>11</sup> Upon further annealing, this concentration is essentially constant, whereas the Fermi-level position continues to rise.

A possible alternative explanation involves the electric charge of the passivating overlayer. This layer contains elemental sulfur.<sup>7</sup> These electronegative atoms on the surface could become negatively charged, which could partly compensate the normally positive surface charge of our *p*-type sample on the as-treated surface. This can explain (in combination with the decreased density of surface states) the low value of the surface barrier on the as-treated surface, and its increase upon desorption of the passivating overlayer. Note the surprisingly high position of the surface Fermi level, at the end of the desorption of the passivating overlayer (annealing run 4). A similar position of the SFL was found recently on the GaAs surface passivated in vacuum using sulfur evaporation after annealing at 450–500 °C.<sup>22</sup> In the present framework, this indicates a large positive value of the surface electric charge, and is not understood in detail.<sup>23</sup>

SFL takes its final position, near midgap, after desorption of As-related surface bonds. This position is very close to the one on a clean surface.<sup>24</sup> Indeed, the desorption of excess arsenic, which occurs after annealing at 360 °C, induces arsenic dimers, and results in a decrease of SRV. This shows very clearly the role of excess arsenic on the surface electronic properties. The present results show that the optimum surface electronic properties are not obtained on the as-treated surface, but on the surface where As-related bonds are broken. For a minimum value of the SRV, it is necessary to reduce as much as possible the excess arsenic concentration produced by the passivation.

The main reason for the degradation of the surface electronic properties under sulfur desorption is due to Ga-related surface defects. Indeed, for an ideal defect-free surface, the disappearance of Ga-S chemical bonds should produce a very small SRV decrease: As verified by calculations,<sup>25</sup> for the clean surface, the effect of reconstruction is to remove the electronic levels away from the band gap, so that gallium dimers should not have a level in the forbidden gap. Thus,

both before and after annealing there does not exist a level in the semiconductor band gap.

The clean (001) surface is by no means such an ideal surface because the SFL is pinned near midgap. It was shown that the fundamental reason for this pinning is intrinsic surface defects which for *p*-type material can be step edges, uncomplete unit cells, etc.<sup>26</sup> We conclude that these defects are passivated by sulfur bonding, and reappear after sulfur desorption which produces a decrease of SRV.

We have qualitatively studied the role of defects on the passivated surface. We first prepared a clean Ga-rich surface, by successive annealings in UHV of As-capped GaAs. This surface was subsequently taken out of UHV, sulfide-passivated and reintroduced into the chamber. The whole procedure took place without exposure to ambient air, in the glovebox connected to the introduction lock of our experimental setup. We repeated this experiment twice, using high-purity *n*-type GaAs, and, respectively, 1*M* and 0.1*M* Na<sub>2</sub>S solutions.

As already found elsewhere,<sup>17</sup> the PLI of the as-treated passivated surfaces increases with the sulfide concentration of the passivating solution. With respect to the PLI of a piece of the same wafer prepared by As-decapping and oxidation in ambient air, we find that 1*M* passivation increases the PLI by a factor of 4.5, whereas, surprisingly, 0.1*M* passivation decreases the PLI by approximately 40%.

We have compared for several annealing stages the PLI of the two passivated samples with that of the As-decapped sample in UHV. Since a large amount of excess As is present on this last sample after the first annealing stages, we limit ourselves here to annealing stages at a higher temperature corresponding to the transition from the arsenic-rich surface to the gallium-rich one. As found from the RA spectra, this manifests itself in the decrease of the arsenic-dimer line and in the appearance of the gallium-dimer one, mostly because of breaking of Ga-S bonds for the S-passivated samples. The results are summarized in Fig. 5, which shows, for each annealing stage, the position of the sample surface in a three-dimensional coordinate frame where the axes are the Ga dimer signal (*x*), the As dimer signal (*y*), and the PLI (*z*).

The PLI of the As-decapped sample is very close to that of the same surface after oxidation in ambient air, which verifies that the former surface contains a significant amount of defects. As expected, the PLI decrease after annealing, probably due to desorption of residual arsenic, is significantly smaller than for the sulfide-passivated samples. One sees that, again, after annealing the PLI of the 0.1*M* passivated surface is smaller than on the As-decapped one.

The PLI decrease upon 0.1*M* Na<sub>2</sub>S passivation shows that this passivation also creates surface defects, probably because of the etching of the surface produced by OH<sup>-</sup> ions.<sup>10</sup> These defects act as recombination centers because due to the smaller sulfur concentration, as found by AES, they are not efficiently passivated. On the other hand, for the 1*M* passivation, these defects are efficiently passivated because the sulfur concentration is larger, which explains the larger PLI.

As discussed elsewhere,<sup>27</sup> RAS allows an independent evaluation of some defect concentration, from the evaluation of the total dimer (Ga+As) concentration. One sees that, in the *xy* frame, the point which represents the surface approxi-

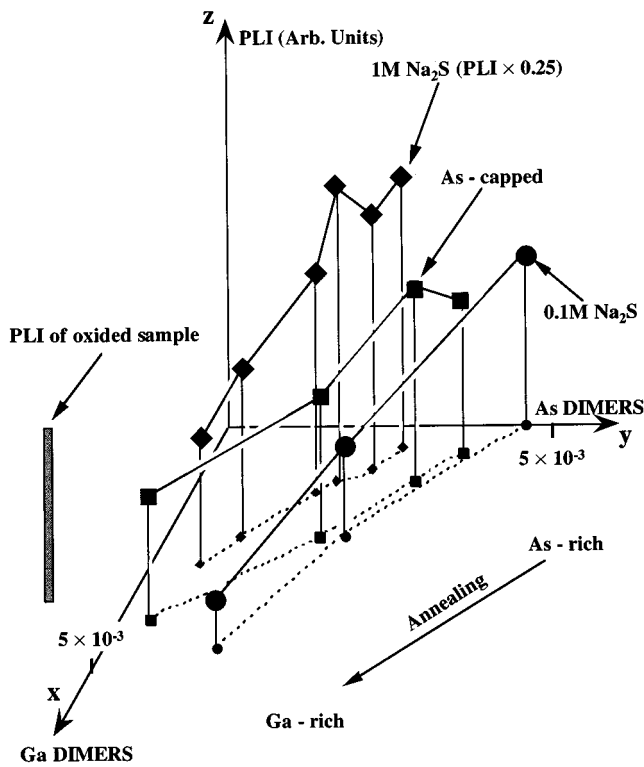


FIG. 5. Photoluminescence intensity as a function of arsenic dimer signal and the gallium dimer signal for different annealing stages. With respect to As-decapped GaAs, passivation by  $1M$   $\text{Na}_2\text{S}$  increases the PLI and decreases the dimer signal. Passivation by  $0.1M$   $\text{Na}_2\text{S}$  has the opposite effect.

mately follows under annealing a straight line. The distance between this line and the origin is connected to the total dimer concentration on the surface, which is smaller if the defect concentration is larger. One sees that this concentration for the  $1M$  passivated sample is smaller than for the sample before passivation, whereas the situation is opposite for the  $0.1M$  passivated sample. This is due to the different defect concentrations on these surfaces, which are then found to be maximum for the  $1M$  passivated sample and minimum for the  $0.1M$  passivated one.

These observations suggest that two different types of surface defects are present. There is first the defects on which depends the SRV, which are only passivated by concentrated

sulfide solutions. These solutions create another type of defect, possibly related with the increased surface roughness, which limits the establishment of surface dimers, but which have a smaller effect on the SRV.

## V. CONCLUSION

We have presented here a correlation between the electronic properties of the sulfur-passivated surface and its chemical properties. For our model system, we have performed a quantitative analysis of the modification of the photoluminescence and photoreflectance upon annealing, from which we obtain the variation of surface recombination velocity and surface barrier. We demonstrate that photoreflectance can be better adapted than photoluminescence because the PLI variation may be very small due to the compensating effect of the photovoltage. Since the effect of this annealing on the chemical bonds on the surface is known from photoemission spectroscopy on the same surface, we were able to demonstrate experimentally the dominant features which determine the quality of the passivation.

Based on the present results, we propose the following description for the change electronic properties of GaAs(001) during passivation: (i) on the gallium-terminated part of (001) surface, Ga-O bonds change to Ga-S bonds which does not induce states in the forbidden gap. Formation of chemical bonds between sulfur and Ga-related surface defects leads to their complete or partial passivation. (ii) At the same time, some accumulation of surface arsenic and formation As-As surface bonds (instead of As-O) takes place. This last fact deteriorates the electronic passivation, and the optimum surface electronic properties can be obtained only after annealing that breaks As-related surface bonds. (iii) Formation of surface defects due to etching of surface in passivating solutions also influences the result of the passivation.

## ACKNOWLEDGMENTS

We are grateful to J.-P. Hirtz of Thomson CSF, for providing the  $p$ -type sample, and to V. Thierry-Mieg for growing the As-capped sample. A.O.G. is grateful to the French Ministère pour l'Enseignement Supérieur et la Recherche (MESR) for financial support. This work was supported by the Russian Fundamental Research Foundation and by a Réseau Formation Recherche of the MESR.

\*On leave from A. F. Ioffe Physico-Technical Institute, 194021 Saint Petersburg, Russia.

<sup>1</sup>B. J. Skromme, C. J. Sandroff, E. Yablonovitch, and T. Gmitter, *Appl. Phys. Lett.* **51**, 2022 (1987).

<sup>2</sup>Y. Wang, Y. Darici, and P. H. Holloway, *J. Appl. Phys.* **71**, 2746 (1992).

<sup>3</sup>C. J. Spindt, R. S. Besser, R. Cao, K. Miyano, C. R. Helms, and W. E. Spicer, *Appl. Phys. Lett.* **54**, 1148 (1989).

<sup>4</sup>R. S. Besser and C. R. Helms, *Appl. Phys. Lett.* **52**, 1707 (1988).

<sup>5</sup>M. S. Carpenter, M. R. Melloch, B. A. Cowans, Z. Dardas, and W. N. Delgass, *J. Vac. Sci. Technol. B* **7**, 845 (1989).

<sup>6</sup>H. Sugahara, M. Oshima, H. Oigawa, and Y. Nannichi, *J. Vac. Sci. Technol. A* **11**, 52 (1993).

<sup>7</sup>K. M. Geib, J. Shin, and C. W. Wilmsen, *J. Vac. Sci. Technol. B* **8**, 838 (1990).

<sup>8</sup>T. Ohno and K. Shiraishi, *Phys. Rev. B* **42**, 11 194 (1990).

<sup>9</sup>C. J. Spindt and W. E. Spicer, in *Proceedings of the Twelfth State-of-the-Art Programme on Compound Semiconductors*, edited by D. C. D'Avanzo, R. E. Enstrom, A. T. Macrander, and D. De-Coster, The Electrochemical Society Proceedings Vol. 90-15 (The Electrochemical Society, Pennington, NJ, 1990), p. 3.

<sup>10</sup>V. L. Berkovits, V. M. Lantratov, T. N. L'vova, G. A. Shakiashvili, V. P. Ulin, and D. Paget, *Appl. Phys. Lett.* **63**, 970 (1993).

<sup>11</sup>D. Paget, J. E. Bonnet, V. L. Berkovits, P. Chiaradia, and J. Avila, preceding paper, *Phys. Rev. B* **53**, 4604 (1996).

<sup>12</sup>H. Shen and F. H. Pollak, *Phys. Rev. B* **42**, 7097 (1990).

- <sup>13</sup>I. Kamiya, D. E. Aspnes, L. T. Florez, and J. P. Harbison, *Phys. Rev. B* **46**, 15 894 (1992).
- <sup>14</sup>V. L. Berkovits, V. N. Bessolov, T. N. L'vova, E. B. Novikov, V. I. Safarov, R. V. Khasieva, and B. V. Tsarenkov, *J. Appl. Phys.* **70**, 3707 (1991).
- <sup>15</sup>V. L. Berkovits and D. Paget, *Appl. Phys. Lett.* **61**, 1835 (1992).
- <sup>16</sup>R. P. Silberstein and F. H. Pollak, *J. Vac. Sci. Technol.* **17**, 1052 (1980).
- <sup>17</sup>R. S. Besser and C. R. Helms, *J. Appl. Phys.* **65**, 4306 (1989).
- <sup>18</sup>X. Yin, H.-M. Chen, H. F. Pollak, Y. Chan, P. A. Montano, P. D. Kirchner, G. D. Pettit, and J. M. Woodall, *Appl. Phys. Lett.* **58**, 261 (1991).
- <sup>19</sup>W. W. Gärtner, *Phys. Rev.* **116**, 84 (1959).
- <sup>20</sup>J. M. Moison, M. Van Rompay, and M. Bensoussan, *Appl. Phys. Lett.* **48**, 1362 (1986), and references therein.
- <sup>21</sup>D. E. Aspnes, *Surf. Sci.* **132**, 406 (1983).
- <sup>22</sup>P. Moriarty, B. Murphy, L. Robers, A. A. Cafolla, G. Hughes, L. Koenders, and P. Bailey, *Phys. Rev. B* **50**, 14 237 (1994).
- <sup>23</sup>If sulfur atoms diffuse underneath the surface under annealing, this results in a superficial compensation of the semiconductor, which could interpret this effect. Although this explanation does not account for the value of the surface barrier after the subsequent annealing stages, it cannot be completely excluded.
- <sup>24</sup>W. Chen, M. Dumas, D. Cao, and A. Kahn, *J. Vac. Sci. Technol. B* **10**, 1886 (1992).
- <sup>25</sup>S.-F. Ren and Y.-C. Chang, *Phys. Rev. B* **44**, 13 573 (1991).
- <sup>26</sup>M. D. Pashley, K. W. Haberern, R. M. Feenstra, and P. D. Kirchner, *Phys. Rev. B* **48**, 4612 (1993).
- <sup>27</sup>D. Paget, V. L. Berkovits, and A. O. Gusev, *J. Vac. Sci. Technol. A* **13**, 2368 (1995).